DOI: 10.1002/chem.200700107

Dinuclear Amine–Thiophenolate Complexes Coligated by Ferrocenemonocarboxylate and 1,1′-Ferrocenedicarboxylate Anions: Preparation, Characterization and Structures of Trinuclear $[LM^{II}_2(O_2CC_5H_4FeCp)]^+$ and Pentanuclear $[(LM^{II}_2)_2(O_2CC_5H_4)_2Fe]^{2+}$ Complexes (M = Co, Ni, Zn)

Vasile Lozan,[a] Axel Buchholz,[b] Winfried Plass,[b] and Berthold Kersting*[a]

Abstract: A series of novel tri- and pentanuclear complexes composed of dinuclear LM_2 units (M = Co, Ni, Zn; L = 24-membered macrocyclic hexaazadithiophenolate ligand) and ferrocenecarboxylate ($[CpFeC_5H_4CO_2]^-$) or 1,1′-ferrocenedicarboxylate ($[Fe(C_5H_4CO_2)_2]^{2-}$) groups is reported. The complexes $[LM^{II}_2(O_2CC_5H_4FeCp)]^+$ (M = Co (**6**), Ni (**7**), Zn (**8**)) and $[(LM^{II}_2)_2(O_2CC_5H_4)_2Fe]^{2+}$ (M = Co (**9**), Ni (**10**)) have been prepared by substitution reactions from labile $[LM^{II}_2L']^+$ precursors (L′ = Cl, OAc) and the respective ferrocenecarboxylate anions in methanol. Mixed-valent $[(LCo^{II}Co^{III})_2(O_2CC_5H_4)_2Fe]^{4+}$ (**11**) was prepared by oxidation of **9** with bromine. Complexes **7**$[BPh_4]$, **8**$[BPh_4]$, **9**$[BPh_4]_2$, **10**$[BPh_4]_2$, and **11**$[ClO_4]_4$ have been characterized by X-ray crystallography; showing that the ferrocenyl carboxylates act as bidentate (**7**, **8**) or bis-bidentate (**9**–**11**) bridging ligands towards one or two bioctahedral LM_2 subunits, respectively. The structures are retained in solution as indicated by NMR spectroscopic studies on the diamagnetic Zn_2Fe complex **8**$[ClO_4]$. Electrochemical studies reveal significant anodic potential shifts for the oxidation potential of the ferrocenyl moieties upon complexation and the magnitude of the potential shift appears to correlate with the charge of the LM_2 subunits. This is qualitatively explained in terms of destabilizing electrostatic (Coulomb) interactions between the M^{2+} ions of the LM_2 unit and the proximate ferrocenium fragment. An analysis of the temperature-dependent magnetic susceptibility data for **10**$[BPh_4]_2$ shows the presence of weak ferromagnetic magnetic exchange interactions between the Ni^{II} ions in the LNi_2 units. The exchange coupling across the ferrocenedicarboxylate bridge is negligible.

Keywords: binuclear complexes · ferrocene · magnetic properties · polynuclear complexes · redox chemistry

Introduction

Polynuclear complexes composed of classical and organometallic complex fragments have attracted considerable attention in recent years,[1,2] owing to their rich redox chemistry,[3,4] the search for novel magnetic and electronic materials,[5,6] and potential applications in catalysis.[7] In addition, the presence of redox-active signalling groups and open coordination sites enables these compounds to be used as selective sensor molecules for target guest species.[8–12] So far, research in this area has mainly focused on conjugates built up of mononuclear LM complexes (L = chelate ligand) and suitably functionalized ferrocene derivatives.[13–16] Less attention has been paid to the use of discrete dinuclear LM_2 building blocks. The tetranuclear Mo_4 complexes containing two quadruply bonded Mo_2 formamidinate units linked by 1,1′-ferrocenedicarboxylate dianions may serve as rather rare examples of this class of compounds.[17]

Recently, we described a series of dinuclear transition-metal complexes supported by the macrocyclic hexaazadithiophenolate ligand L^{2-} (Scheme 1). These complexes have a rich coordination chemistry since the $[LM_2]^{2+}$ fragments are able to coordinate a large variety of coligands such as

---

[a] Dr. V. Lozan, Prof. Dr. B. Kersting
Institut für Anorganische Chemie, Universität Leipzig
Johannisallee 29, 04103 Leipzig (Germany)
Fax: (+49) 341-973-6199
E-mail: b.kersting@uni-leipzig.de

[b] Dr. A. Buchholz, Prof. Dr. W. Plass
Institut für Anorganische und Analytische Chemie
Friedrich-Schiller Universität Jena, Carl-Zeiss-Promenade 10
07745 Jena (Germany)

Supporting information for this article is available on the WWW under http://www.chemeurj.org/ or from the author.

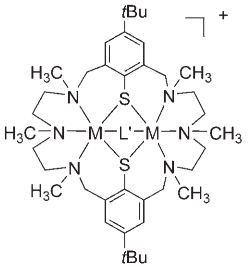

$[LM^{II}_2(L')]^+$

1: $[LCo^{II}_2(Cl)]^+$
2: $[LNi^{II}_2(Cl)]^+$
3: $[LZn^{II}_2(OAc)]^+$
4: $[LCo^{II}_2(OAc)]^+$
5: $[LNi^{II}_2(OAc)]^+$

Scheme 1. Dinuclear complexes of the hexaaza-dithiophenolate ligand L^{2-}.

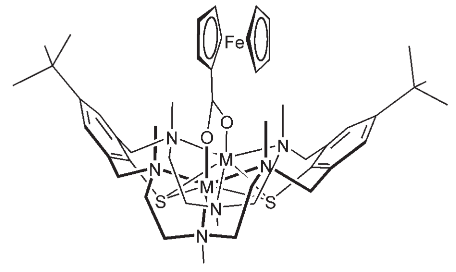

6: $[LCo^{II}_2(O_2CC_5H_4FeCp)]^+$
7: $[LNi^{II}_2(O_2CC_5H_4FeCp)]^+$
8: $[LZn^{II}_2(O_2CC_5H_4FeCp)]^+$

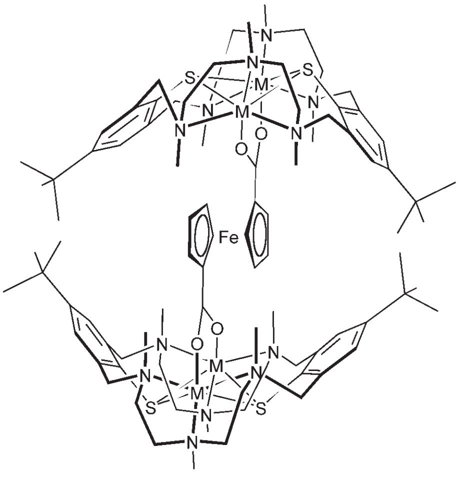

9: $[(LCo^{II}_2)_2(O_2CC_5H_4)_2Fe]^{2+}$
10: $[(LNi^{II}_2)_2(O_2CC_5H_4)_2Fe]^{2+}$
11: $[(LCo^{II}Co^{III})_2(O_2CC_5H_4)_2Fe]^{4+}$

Scheme 2. Complexes prepared and their labels.

Cl^-,[18] OH^-,[19] NO_2^-, NO_3^-, N_3^-,[20] BH_4^-,[21] and various carboxylates.[22–24] The extensive redox chemistry exhibited by these dinuclear amine–thiolate complexes[25] and the possibility of coupling these units into polynuclear arrays, led us to synthesize derivatives bearing ferrocenemono- and ferrocenedicarboxylate anions ($[CpFeC_5H_4CO_2]^-$ and $[Fe(C_5H_4CO_2)_2]^{2-}$, Cp = cyclopentadienyl) as coligands. Our first attempts afforded a series of trinuclear $[LM_2(O_2CC_5H_4FeCp)]^+$ and pentanuclear $[(LM_2)_2(O_2CC_5H_4)_2Fe]^{2+}$ complexes. Their preparation, crystal structure determination, spectroscopic, magnetic, and electrochemical properties are reported here. To our knowledge, these complexes represent the first class of compounds containing dinuclear aminethiolate complexes and redox-active ferrocenecarboxylates in the same molecule.[26–28]

Results and Discussion

Syntheses and characterization: It was our aim to synthesize polynuclear complexes containing classical and organometallic complex fragments. Two types of complexes were considered: trinuclear $[LM^{II}_2(O_2CC_5H_4FeCp)]^+$ complexes and pentanuclear $[(LM^{II}_2)_2(O_2CC_5H_4)_2Fe]^{2+}$ compounds (hereafter abbreviated as M^{II}_2Fe and M^{II}_4Fe), respectively. Scheme 2 shows the complexes prepared and their labels.

The trinuclear Co_2Fe and Ni_2Fe complexes, **6** and **7**, were obtained in almost quantitative yield by reaction of the corresponding chloride complex $[LM_2(\mu\text{-}Cl)]^+$ (M = Co **1**, Ni **2**) with triethylammonium ferrocenylmonocarboxylate (prepared in situ from $CpFeC_5H_4CO_2H$ and triethylamine) in a 1:3 ratio in methanol at room temperature and isolated as perchlorate salts upon addition of $LiClO_4$. It should be noted that these reactions are not simple substitution reactions, because a simultaneous conformational change of the supporting ligand from a "partial-cone" to a "bowl-shaped" conformation takes place.[29] Since a chloro-bridged dizinc complex $[LZn^{II}_2(\mu\text{-}Cl)][ClO_4]$ is not yet known, the synthesis of the Zn_2Fe complex **8**$[ClO_4]$ required another starting material. Complex $[LZn^{II}_2(\mu\text{-}OAc)][ClO_4]$ (**3**$[ClO_4]$) was chosen due to its proven ability to readily exchange its acetato group for more hydrophobic carboxylate anions.[24] Indeed, when **3**$[ClO_4]$ is treated with a 10-fold excess of triethylammonium ferrocenecarboxylate in methanol at room temperature an exchange reaction takes place and **8**$[ClO_4]$ can be isolated as an analytically pure yellow powder after workup. The three perchlorate salts **6**$[ClO_4]$–**8**$[ClO_4]$ are air-stable solids that are readily soluble in polar aprotic organic solvents such as dimethylformamide, dichloromethane, acetone and acetonitrile but only slightly soluble in methanol or ethanol. The corresponding tetraphenylborate salts **6**$[BPh_4]$–**8**$[BPh_4]$ are formed within a few minutes upon addition of ethanol solutions of $NaBPh_4$ to acetonitrile solutions of the ClO_4^- salts.

The pentanuclear Ni^{II}_4Fe and Co^{II}_4Fe complexes $[(LM_2)(\mu\text{-}O_2CC_5H_4)_2Fe]^{2+}$ (M = Co (**9**), Ni (**10**)) were prepared in much the same way as **6** and **7**: the chloride complexes **1** and **2** reacted smoothly with half an equivalent of triethylammonium 1,1′-ferrocenedicarboxylate (prepared in situ from the free acid and triethylamine) in methanol to give red-brown **9**$[ClO_4]_2$ and green **10**$[ClO_4]_2$, respectively, in nearly quantitative yields. The coupling of the dicarboxylate dianions with the $[LM_2]^{2+}$ fragments is a clean and facile step driven forward by the low solubility of the products. The complexes are only slightly soluble in polar aprotic organic solvents such as DMF, dichloromethane, and acetonitrile and virtually insoluble in methanol or ethanol. Addition of $NaBPh_4$ to suspensions of the perchlorate salts in acetonitrile/ethanol followed by concentration in vacuum provided the corresponding tetraphenylborate salts as analytically pure products.

We have also been able to isolate the two-electron-oxidized $Co^{II}Co^{III}$ form **11**$[ClO_4]_4$ of compound **9**$[ClO_4]_2$. This mixed-valent complex was prepared as a black powder in good yields by oxidation of **9**$[ClO_4]_2$ with 1 equiv of bromine in acetonitrile at 0 °C followed by addition of a saturated ethanol solution of $LiClO_4$ and low-temperature vacuum concentration. In contrast to **9**$[ClO_4]_2$, **11**$[ClO_4]_4$ exhibits excellent solubility in acetonitrile. Such solutions can be stored for several days at ambient temperature without noticeable decomposition. Attempts to prepare the analogous $[(LNi^{II}Ni^{III})_2(\mu\text{-}O_2CC_5H_4)_2Fe]^{4+}$ complex were not successful.

All compounds gave satisfactory elemental analyses and were characterized by appropriate spectroscopic methods (IR, NMR, UV/Vis spectroscopy). The infrared spectra of the new complexes display absorptions due to the $[LM_2]^{2+}$ fragments, the counter ions (ClO_4^- or BPh_4^-), and the ferrocene derivatives. The ferrocenecarboxylates in **6**–**10** give rise to two characteristic bands, as in other carboxylato-complexes,[30,31] in the 1575–1565 cm^{-1} and 1435–1425 cm^{-1} ranges; these are assigned to the asymmetric and symmetric carboxylate stretching modes, respectively. These values are very similar to those in **3**–**5** indicative of $\mu_{1,3}$-bridging carboxylate functions.[22,23] The oxidation of **9** to **11** is accompanied by a shift of the asymmetric stretching mode by $\approx 18\ cm^{-1}$ to lower wavenumbers. A similar behaviour was observed for the acetato-bridged Co^{II}_2 complex **4**.[23] The data are thus in good agreement with the formulation of complex **11** as a mixed-valent $Co^{II}Co^{III}$ species.

The diamagnetic Zn_2Fe complex **8** was characterized by NMR spectroscopy to determine its structure in solution. The ^1H NMR spectrum shows the characteristic signal patterns for the $[LZn_2]^{2+}$,[32] and $[CpFe(C_5H_4CO_2)]^-$,[33] units indicating local C_{2v} symmetry for **8**. Particularly indicative of a stable 1:1 complex is the upfield shift of the *tert*-butyl resonance of the LZn_2 unit (0.25 ppm relative to **3**). The resonances of the ferrocenecarboxylate are observed at δ 3.40 for the unsubstituted Cp ring, δ 3.90 for the two *meta* H and δ 4.04 for the two *ortho*-H of the substituted Cp ring. These values are also significantly shifted to higher field when compared with the corresponding resonances of uncomplexed ferrocenmonocarboxylate.[34,35] The ^{13}C NMR spectrum is also in accord with the proposed formulation showing five signals for the $[CpFe(C_5H_4CO_2)]^-$ unit and only 13 signals for the $[LZn_2]^{2+}$ moiety. The local C_{2v} symmetry is suggestive of a dynamic averaging process in solution. A rapid rotation of the ferrocenyl group about the CpFeCp–CO_2Zn_2L bond seems most likely. This motion would result in the coalescence of the respective signals and the time-averaged C_{2v} symmetry of the complex. The crystal structure determinations of **6** and **7** support this assumption.

The UV/Vis spectra of **6**, **7**, **9**, and **10** display several weak bands above 500 nm typical of octahedral high-spin Co^{II} (d^7, $S=3/2$) and Ni^{II} (d^8, $S=1$) ions, respectively. The observed values closely compare with those of **4** and **5** again consistent with pseudo-octahedral N_3S_2O coordination environments around the metal atoms.[22,23] For the Zn_2Fe species **8**$[ClO_4]$ two absorptions bands are detected at 342 and 440 nm; these are readily assigned to the d–d transitions of the coordinated $[CpFe(C_5H_4CO_2)]^-$ unit. The feature at 440 nm is also evident in the electronic absorption spectrum of the Ni_2Fe complex **7**. In the UV spectrum of **8**, this band is obscured by an intense ligand-to-metal charge-transfer transition ($RS^- \rightarrow Co^{II}$). The d–d transitions of the $[Fe(\eta^5\text{-}C_5H_4CO_2)]^{2-}$ unit in **9**, **10** and **11** could not be located.

The UV/Vis spectrum of the mixed-valent $Co^{II}Co^{III}$ complex **11** is dominated by two very intense absorptions at ≈ 449 and 681 nm; these are attributable to $RS^- \rightarrow Co^{III}$ charge-transfer transitions. Such intense LMCT transitions are characteristic of thiolato-bridged $Co^{II}Co^{III}$ complexes. The corresponding absorptions in $[LCo^{II}Co^{III}(\mu\text{-}OAc)]^{2+}$, for example, were observed at 460 and 710 nm.[23] It should be noted that the UV/Vis spectrum of **11** reveals no bands attributable to intervalence transfer (IT) bands. Complex **11** is therefore presumably class I in Robin and Day's classification of mixed-valence species with distinct localized high-spin Co^{II} and low-spin Co^{III} sites.[36] This is confirmed by the crystal structure determination of **11**$[ClO_4]_4$.

Description of crystal structures

6[BPh$_4$]·3MeCN: Crystals of **6**$[BPh_4]\cdot 3MeCN$ suitable for X-ray crystallography were grown by slow evaporation of a dilute 1:1 acetonitrile/ethanol solution of **6**$[BPh_4]$. The X-ray structure revealed the presence of well-separated $[LCo^{II}_2(\mu\text{-}O_2CC_5H_4FeCp)]^+$ cations, tetraphenylborate anions, and acetonitrile molecules of solvent of crystallization. An ORTEP representation of the molecular structure of **6** is shown in Figure 1. Table 1 lists selected bond lengths and angles.

The ferrocenecarboxylate bridges the two Co atoms in a $\mu_{1,3}$-fashion, resulting in nonbonded Co···Fe separations of 5.884(1) and 5.753(1) Å. The Co···Co distance of 3.448(1) Å is the same as that in **4**.[23] The Cp rings are nearly parallel (angle between the normals of the Cp planes = 1.8(1)°) and adopt an almost eclipsed conformation, with the torsional angle τ (defined as "CO$_2$-centroid-centroid-C(45)") being 6.4(1)°. The carboxylato plane is slightly twisted by 9.7° with respect to the Cp ring to which it is attached. The Fe–centroid distances are 1.656(6) and 1.646(6) Å for the carboxylated and the unsubstituted Cp rings, respectively; the mean Fe–ring(centroid) distance of 1.651(6) Å is, within experimental error, the same as that of 1.645(2) Å for ferrocene.[37] The bond lengths and angles around the Co atoms within the $[LCo^{II}_2]^{2+}$ unit reveal no unusual features. The average Co–S, Co–N and Co–O bond lengths are at 2.018(3), 2.291(3), and 2.517(1) Å, respectively. Virtually the same distances are seen in the acetato-bridged complex **4**.[23] A

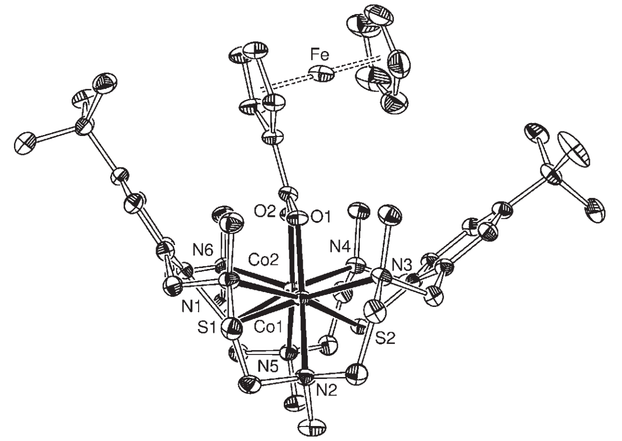

Figure 1. Structure of the cation **6** in crystals of **6**$[\mathrm{BPh}_4]\cdot 3\,\mathrm{MeCN}$. Thermal ellipsoids are drawn at the 30% probability level. Hydrogen atoms are omitted for reasons of clarity. Only one orientation of a rotationally disordered *t*Bu group is shown.

large number of metal complexes containing ferrocenecarboxylate ligands have been structurally characterized;[38–40] to our knowledge, **6** is the first such complex supported by a dinuclear aminethiolate metallo ligand.

Compound 7[BPh$_4$]·MeCN: In contrast to the compound above, **7**[BPh$_4$] recrystallized from acetonitrile/ethanol 1:1 with only one acetonitrile solvate molecule. Figure 2 shows the ferrocenecarboxylate to be coordinated to the $[\mathrm{LNi^{II}}_2]$ unit in a manner identical to the situation found in **6** (Figure 2). Thus, both Ni$^{\mathrm{II}}$ ions are six coordinate with three N and two S atoms from L^{2-} and one O atom of a $\mu_{1,3}$-bridging ferrocenyl carboxylate group. In comparison to **6**, the two Cp rings are perfectly eclipsed (tilt angle = 0.6(1)°) and the carboxylato plane is now coplanar with the Cp ring ($\tau = 2.8°$). The different τ values may be taken as evidence for an unhindered rotation of the coordinated ferrocene moiety about the O$_2$C–Cp bond in the solution state. It should be noted in this respect that there are no intramolecular steric interactions between the ferrocene group and the *t*Bu substituents. The short distances between C(45) and the π-electrons of the adjacent phenyl ring (d(C45)···centroid = 3.518 Å in **7** and 3.991 Å in **6**) may be considered as weak CH···π hydrogen bonds. The Ni–O, Ni–N, and Ni–S distances of the [LNi$_2$carboxylate] subunit in **7** are unexceptional and are very close to the corresponding distances in **5**. Overall, the two structures clearly show that the $[\mathrm{LM}_2]^{2+}$ units can expand their binding pockets sufficiently to accommodate $\mu_{1,3}$-bridging ferrocenecarboxylate ions.

Compound 9[BPh$_4$]$_2$·2^2/$_3$MeCN·^{1}/$_3$H$_2$O and 10[BPh$_4$]$_2$·1.75MeCN·EtOH·0.25H$_2$O: Single crystals of the two title compounds suitable for X-ray crystallography were each obtained by slow evaporation from an acetonitrile/ethanol/CH$_2$Cl$_2$ solution. The crystal structures consist of isolated $[(\mathrm{LM}_2)_2(\mathrm{O_2CC_5H_4})_2\mathrm{Fe}]^{2+}$ dications (Figure 3), tetraphenylborate anions and various solvate molecules (MeCN, H$_2$O, and EtOH), of which some are either severely disordered or not fully occupied (see Experimental Section). The two compounds were found to be isomorphous in spite of differences in the number and type of solvate molecules. The following discussion will focus on the Co$^{\mathrm{II}}_4$Fe complex **9**. Metrical details for the Ni$_4^{\mathrm{II}}$Fe complex **10** are reported in square brackets.

As can be seen in Figure 3b, the ferrocenyldicarboxylate dianion links two $[\mathrm{LCo^{II}}_2]^{2+}$ units via two $\mu_{1,3}$-bridging carboxylate functions. The $[\mathrm{LCo}_2]^{2+}$ subunits in **9** and **4** are structurally very similar, and the Co–N, Co–O, and Co–S distances lie within very narrow ranges (see Table 1). The carboxylato groups on the Cp rings assume an *anti*-eclipsed conformation as manifested by a torsional angle τ (CO$_2$-centroid-centroid-CO$_2$) of 148.4° [148.3°]. The distance d between the centre of the Co···Co axes of the binuclear subunits amounts to 10.751 Å [10.749 Å], which is slightly smaller than the corresponding distance in $[\mathrm{Mo_2(DAniF)_3}]_2$[ferrocendicarboxylate].[17] It should be noted that the Co$_2$carboxylato planes are considerably tilted against each other (32.3°, [33.1°]) and also with respect to their corresponding Cp rings (22.4°, 10.1°; [22.4°,10.0°]). This distortion from coplanarity relates to steric interactions between the *t*Bu groups of the two opposing $[\mathrm{LCo^{II}}_2]^{2+}$ subunits. The *tert*-butyl groups must interlock to accommodate the dicarboxylate ion. In ferrocenedicarboxylato complexes of sterically less encumbered supporting ligands the carboxylato planes are both coplanar with their parent Cp rings.[41,42]

Compound 11[ClO$_4$]$_2$·4H$_2$O: The crystal structure of **11**-[ClO$_4$]$_4$·4H$_2$O consists of $[(\mathrm{LCo^{II}Co^{III}})_2(\mu\text{-}\mathrm{O_2CC_5H_4})_2\mathrm{Fe}]^{4+}$ cations (Figure 4), ClO$_4^-$ anions and water solvate molecules. There are two crystallographically independent but chemically almost identical molecules (labelled A and B) in the asymmetric unit; both have crystallographically imposed C_2 symmetry with the iron atoms residing on crystallographic two-fold axes. The overall structure of complex **11** is very similar to that of its parent **9**, featuring two binuclear LCo$_2$ subunits linked by a tetradentate ferrocenedicarboxylate ion. Again, the carboxylato groups are *anti*-eclipsed (τ = 148.6° [136.9° (molecule B)] and considerably tilted against each other (48.2°, [25.2°]) and by 24.1° [12.6°] with respect to their corresponding Cp rings. The distance d between the centre of the Co···Co axes is 10.770 Å in molecule A and 10.322 Å in molecule B.

The oxidation of **9** to **11** is accompanied by a significant shortening of the metal–ligand bond lengths around one Co atom in each binuclear subunit. This is in accord with the mixed-valent nature of **11** and the metal-centred nature of the oxidation of **9**. Assignments of the trivalent and divalent Co ions are based on the bond distances around the cobalt atoms. Co1a [Co1b in molecule B] is assigned an oxidation state +II (d^7, high-spin), because the bond lengths are very similar to those in **9**. The average Co–O, Co–N and Co–S bond lengths around Co2a [Co2c] are all significantly shorter at 1.884(4), 2.122(6), and 2.311(2) Å, respectively. These distances are too short for a six-coordinate Co$^{\mathrm{II}}$ complex,

Table 1. Selected bond lengths [Å] and angles [°] for the complexes reported in this study.

	6 (M=Co)	**5** (M=Ni)	**7** (M = Co)[b]	**8** (M = Ni)[b]	**9** (M1 = Co^{II}, M2 = Co^{III})[c]
M1−O1	2.011(3)	2.021(5)	2.036(5) [2.027(5)]	2.025(2) [2.024(2)]	2.038(4) [2.075(4)]
M1−N1	2.392(3)	2.323(5)	2.344(6) [2.318(7)]	2.326(3) [2.293(3)]	2.248(6) [2.229(6)]
M1−N2	2.217(3)	2.168(6)	2.232(7) [2.205(7)]	2.188(3) [2.187(3)]	2.202(6) [2.214(6)]
M1−N3	2.291(3)	2.233(5)	2.225(7) [2.309(7)]	2.208(3) [2.241(3)]	2.205(6) [2.183(6)]
M1−S1	2.550(1)	2.503(2)	2.503(3) [2.516(2)]	2.478(1) [2.485(1)]	2.561(2) [2.584(2)]
M1−S2	2.471(1)	2.408(2)	2.491(2) [2.485(3)]	2.453(1) [2.445(1)]	2.481(2) [2.448(2)]
M−L[a]	2.322(3)	2.276(4)	2.305(5) [2.310(5)]	2.280(2) [2.279(2)]	2.289(4) [2.289(4)]
M2−O2	2.025(3)	2.016(5)	2.001(5) [2.001(6)]	2.001(2) [1.994(2)]	1.895(4) [1.872(4)]
M2−N4	2.291(3)	2.218(5)	2.302(7) [2.293(7)]	2.255(3) [2.237(3)]	2.118(6) [2.133(6)]
M2−N5	2.196(3)	2.176(5)	2.181(7) [2.216(7)]	2.172(3) [2.188(3)]	2.025(6) [2.038(6)]
M2−N6	2.361(3)	2.298(5)	2.319(7) [2.326(7)]	2.282(3) [2.284(3)]	2.211(5) [2.208(5)]
M2−S1	2.551(2)	2.512(2)	2.518(2) [2.539(3)]	2.482(1) [2.522(1)]	2.339(2) [2.336(2)]
M2−S2	2.495(1)	2.417(2)	2.478(3) [2.470(2)]	2.450(1) [2.427(1)]	2.294(2) [2.274(2)]
M−O[a]	2.018(3)	2.019(5)	2.019(5) [2.014(6)]	2.013(2) [2.009(2)]	
M−N[a]	2.291(3)	2.236(5)	2.267(7) [2.278(7)]	2.239(3) [2.238(3)]	
M−S[a]	2.517(1)	2.460(2)	2.498(3) [2.503(3)]	2.466(1) [2.470(1)]	
M−L[a]	2.320(3)	2.273(4)	2.300(5) [2.308(5)]	2.274(2) [2.275(2)]	2.147(4) [2.144(4)]
C(39)−O1	1.267(4)	1.264(8)	1.270(10) [1.235(9)]	1.257(4) [1.262(4)]	1.252(7) [1.245(7)]
C(39)−O2	1.265(4)	1.242(8)	1.270(10) [1.274(9)]	1.267(4) [1.261(4)]	1.277(7) [1.267(7)]
C(39)−C(40)	1.488(5)	1.515(10)	1.505(11) [1.506(11)]	1.490(4) [1.490(5)]	1.476(9) [1.498(8)]
Fe−C[a]	2.043(6)	2.042(11)	2.028(9)	2.043(4)	2.046(7) [2.043(7)]
M1•••Fe	5.884(1)	5.763(1)	5.762(1) [5.759(1)]	5.752(1) [5.762(1)]]5.741(1) [5.834(1)]	
M2•••Fe	5.753(1)	5.760(1)	5.973(1) [5.807(1)]5.984(1) [5.816(1)]5.907(1) [5.738(1)]		
M1•••M2	3.448(1)	3.485(1)	3.441(1) [3.445(1)]3.479(1) [3.483(1)]3.523(1) [3.518(1)]		
O-M-N_{cis}[a]	87.5(1)	88.0(2)	87.7(2) [86.9(2)]	88.2(1) [87.5(1)]	87.9(2) [91.7(2)]
O-M-N_{trans}[a]	160.6(1)	163.0(2)	160.0(3) [158.0(3)]	162.9(1) [161.3(1)]	167.5(2) [167.8(2)]
S-M-N_{cis}[a]	93.9(1)	94.6(2)	94.0(2) [94.6(2)]	94.35(8) [94.80(8)]	92.4(2) [96.2(2)]
S-M-N_{trans}[a]	170.2(1)	169.0(2)	168.8(2) [168.6(2)]	168.74(8) [168.34(8)]	170.2(2) [165.0(2)]
S-M-S[a]	81.24(4)	78.55(6)	80.31(8) [80.21(8)]	78.81(3) [78.66(3)]	80.61(7) [72.78(6)]
S-M-O[a]	96.2(1)	94.6(2)	96.4(2) [96.4(2)]	94.70(7) [94.87(7)]	94.6(1) [89.9(1)]
N-M-N[a]	86.7(1)	87.4(2)°	87.0(3) [86.9(3)]	87.5(1) [87.6(1)]	89.3(2) [88.0(2)]
M-S-M	86.52(5)	90.27(6)	87.07(8) [87.00(8)]	89.75(3) [89.71(4)]	93.56(7)

[a] Average values. [b] Numbers in parentheses correspond to atoms labelled "b". [c] There are two crystallographically independent molecules A and B in the asymmetric unit. Values in square bracket refer to molecule B.

but are in excellent accord with those of related low-spin $Co^{III}N_{6-x}S_x$[43,44] and $Co^{III}N_3S_2O$[23] complexes. Interestingly, the oxidation of **9** is accompanied by an opening up of the Co-S-Co angle to 93.56(7)° causing a slight increase of the intramolecular Co•••Co distance to 3.523(1) Å. The Fe-Cp-ring(centroid) distances (1.653(6) Å and 1.651(6) Å) are not affected by the oxidation.

Evidently, the crystal structures of **9**–**11** clearly show that dinuclear LM_2 units can be coupled together by the 1,1′-ferrocendicarboxylate dianion. Moreover, the pentanuclear Co_4Fe complex **9** is even accessible in another oxidation state. The oxidation is metal-centered and occurs without gross structural changes of the parent complex **9**. This finding paves the way for novel multi-redox systems composed of binuclear complex units and multifunctional metalorganic linkers which may find applications due to novel chemical or physico-chemical properties that are not seen for the individual components.[45]

Electrochemistry: One facet of the present complexes is the presence of a redox-active ferrocene unit in close proximity to one or two redox-active $[LM_2]^{2+}$ groups. This feature suggests that electron transfer events can influence one another owing to the short distance (5.6 ± 0.2 Å) between the redox centres. To determine whether this is the case, cyclovoltammetric studies have been carried out on the M_2Fe complexes **6**[ClO_4]–**8**[ClO_4] and the Co_4Fe compound **11**[ClO_4]$_4$. The cyclic voltammograms (CV's) have been recorded in acetonitrile solution with tetra-*n*-butylammonium hexafluorophosphate as the supporting electrolyte.

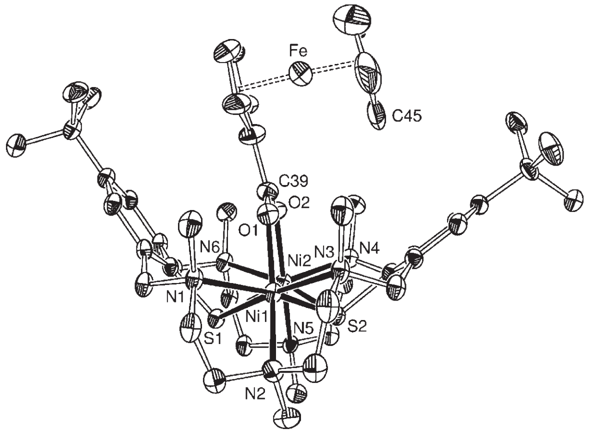

Figure 2. Structure of the cation **7** in crystals of $\mathbf{7}[BPh_4]\cdot MeCN$. Thermal ellipsoids are drawn at the 30 % probability level. Hydrogen atoms are omitted for reasons of clarity. Only one orientation of a rotationally disordered *t*Bu group is shown.

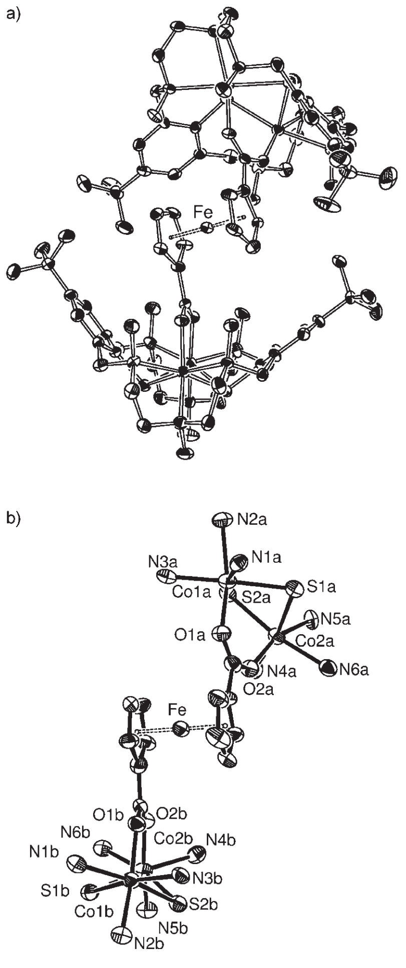

Figure 3. a) ORTEP view of the $[(LCo^{II}_2)_2(\mu\text{-}O_2CC_5H_4)_2Fe]^{2+}$ dication **9** in crystals of $\mathbf{9}[BPh_4]_2\cdot 2\tfrac{2}{3}MeCN\cdot\tfrac{1}{3}H_2O$. Hydrogen atoms are omitted for clarity. b) ORTEP representation of the core structure of **9** with the atom labelling scheme. Ellipsoids are represented at the 30 % probability level.

The electrochemical results are shown in Figure 5, and the redox potentials referenced versus SCE are collected in Table 2. The electrochemical data of **3**–**5**, ferrocenecarboxylic acid and 1,1′-ferrocenedicarboxylic acid have been included for comparative purposes.[46]

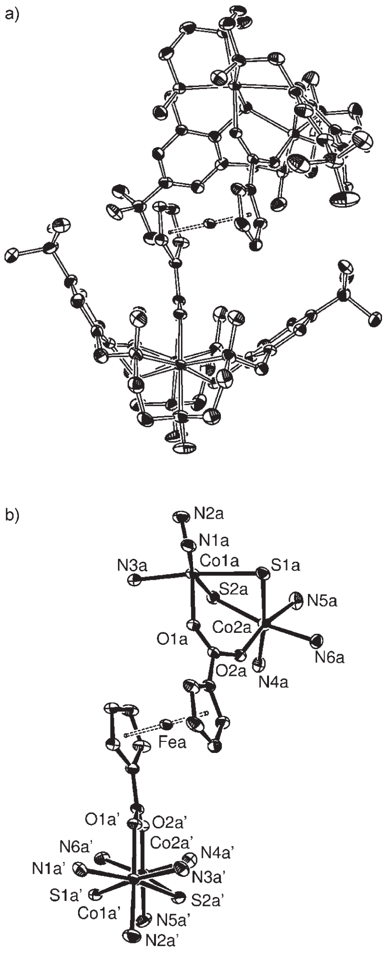

Figure 4. a) ORTEP view of the $[(LCo^{III}Co^{II})_2(\mu\text{-}O_2CC_5H_4)_2Fe]^{4+}$ tetracation (molecule A) in crystals of $\mathbf{11}[ClO_4]_2\cdot 4H_2O$. Hydrogen atoms are omitted for clarity. b) ORTEP representation of the core structure of **11** with the atom labelling scheme. Ellipsoids are drawn at the 30 % probability level. Symmetry code used to generate equivalent atoms: $1-x$, y, $1.5-z$ (′).

The CV of the Zn_2Fe complex $\mathbf{8}[ClO_4]$ shows one reversible redox wave at +0.54 V that can be readily assigned to the oxidation of the ferrocene moiety, since it its absent in the CV of $[LZn_2(OAc)][ClO_4]$ ($\mathbf{3}[ClO_4]$). Interestingly, the complexation of $[CpFe(C_5H_4COO)]^-$ causes an anodic potential shift of 90 mV in the reversible redox wave of the ferrocene moiety. It is assumed that this potential shift results from the electrostatic repulsion (Coulomb) effect between the two Zn^{2+} ions bonded by the macrocycle and the positively charged ferrocenium centre. Thus complexation of $[CpFe(C_5H_4COO)]^-$ by the dipositively charged $[LZn_2]^{2+}$ unit makes the ferrocenyl group more difficult to oxidize. Curiously, an anodic shift of ≈140 mV for the peak potential for the second, irreversible ligand-based oxidation (formally a $RS^- \rightarrow RS^\bullet$ transition)[25] that follows the ferrocenyl-centred oxidation is also evident. In this case it is the additional positive charge on the ferrocene that causes the thio-

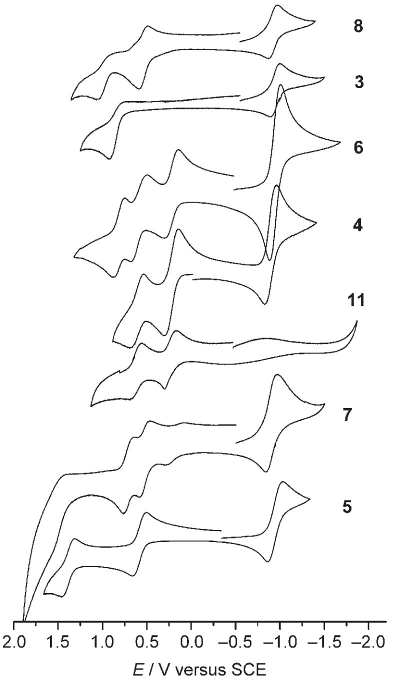

Figure 5. Cyclic voltammograms of the perchlorate salts of complexes **3**–**8** and **11** in CH_3CN solution at 295 K. Experimental conditions: 0.1 M $[nBu_4N][PF_6]$ supporting electrolyte, ca. 1×10^{-3} M sample concentration, Pt disk working, Pt wire auxiliary electrodes, Ag wire reference electrode, scan rate = 100 mV s^{-1}. $[Co(Cp)_2][PF_6]$ internal standard ($E[CoCp_2^+/CoCp_2] = -0.94$ V versus SCE).

late sulfur atoms to be oxidized at a higher potential. The redox-processes for **8**$[ClO_4]$ are summarized in Scheme 3.

The CV of the Co_2Fe complex **6** exhibits three reversible one-electron redox waves which can be assigned to i) a metal-centered $Co^{II}Co^{II}\rightarrow Co^{II}Co^{III}$ oxidation yielding the mixed-valent dication $[LCo^{III}Co^{II}(O_2CC_5H_4FeCp)]^{2+}$ (**6**$^{2+}$) at 0.20 V, ii) a metal-centered $Co^{III}Co^{II}\rightarrow Co^{III}Co^{III}$ oxidation at 0.59 V forming tricationic $[LCo^{III}_2(O_2C_5H_4FeCp)]^{3+}$ (**6**$^{3+}$), and iii) oxidation of the metalorganic unit generating tetracationic $[LCo^{III}_2(O_2CC_5H_4Fe^{III}Cp)]^{4+}$ (**6**$^{4+}$) at 0.81 V. These assignments are supported by the electronic absorption spectra of the corresponding di-, tri- and tetracations generated in situ by successive chemical oxidations of **6**$^+$ with 0.5, 1.0, and 1.5 equiv of bromine in acetonitrile solution (Figure 6); the characteristic absorption maxima at 388 and 467 nm of the ferrocinium ion are not observed before the third oxidation step.

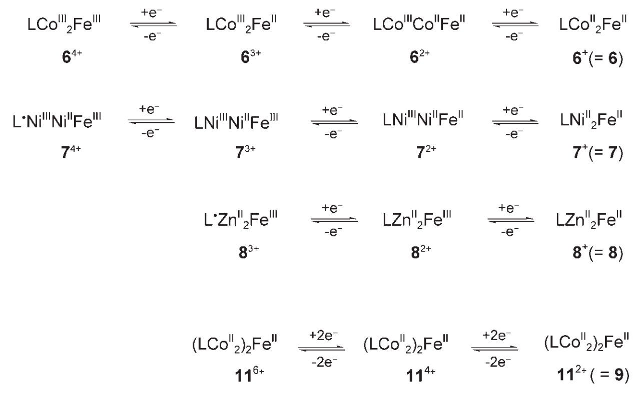

Scheme 3. Assignment of redox processes in **6**–**8** and **11**.

The potential shift for the oxidation of the ferrocenyl unit in **6**$^{3+}$ ($\Delta E = +0.37$ V) is significantly larger than in **8**$^+$. The significantly larger shift is likely to be a result of the higher positive charge of the $[LCo^{III}_2]^{5+}$ fragment to which the $Fe^{II}(Cp)(C_5H_4COO^-)$ unit is attached in **6**$^{3+}$.

The CV of Ni_2Fe compound **7** reveals two electrochemically reversible and one irreversible redox waves, which by comparison with the CV of **5**[25] are tentatively assigned to i) a metal-centred $Ni^{II}Ni^{II}\rightarrow Ni^{II}Ni^{III}$ oxidation yielding the mixed-valent dication $[LNi^{III}Ni^{II}(O_2CC_5H_4Fe^{II}Cp)]^{2+}$ (**5**$^{2+}$) at 0.53 V, ii) the oxidation of the metal organic unit forming $[LNi^{III}Ni^{II}(O_2CC_5H_4Fe^{III}Cp)]^{3+}$ (**5**$^{3+}$) at 0.71 V, and iii) the oxidation of the thiophenolate sulfur atoms yielding a nickel-bound thiyl radical at 1.59 V. Anodic shifts in the second and third redox waves are clearly discernible, confirming the above findings that the electron transfer events of the ferrocenyl moiety and the binuclear subunit influence one another. The fact that the potential shifts are not so pronounced than in **6** is in good agreement with the smaller positive charges of the participating species. It should be noted that all oxidation products of **6** and **7** are only

Table 2. Electrochemical sata, E [V] vs SCE, for the compounds examined in this study.[a]

compound	Solvent	$E_{1/2}$ [V] (ΔE_p [mV])[b]				Ref.
		Fe^{III}/Fe^{II}	$M^{III}M^{II}/M^{II}_2$	$M^{III}_2/M^{III}M^{II}$	$RS^-/RS^{\bullet}$	
3·$Zn_2(OAc)$	CH_3CN				0.92 (irr.)[d]	[25]
4·$Co_2(OAc)$	CH_3CN		0.22 (118)	0.60 (147)		[25]
5·$Ni_2(OAc)$	CH_3CN		0.56 (140)	1.36 (140)		[25]
6·Co_2Fe	CH_3CN	0.81 (120)	0.20 (150)	0.59 (170)		this work
7·Ni_2Fe	CH_3CN	0.55 (120)	0.74 (120)	1.54 (irr.)[d]		this work
8·Zn_2Fe	CH_3CN	0.54 (100)			1.06 (irr.)[d]	this work
11·$Co^{II}_2Co^{III}_2Fe$	CH_3CN	obsc.	0.23 (140)	0.61 (120)		this work
	DMF	obsc.	0.17 (120)	0.52 (120)		this work
$[FeCp_2]$	CH_3CN	0.40				[52]
$[CpFe(C_5H_4CO_2H)]$	aq. CH_3CN	0.53				[46]
	CH_3CN	0.63 (50)				this work
$[CpFe(C_5H_4CO_2)]^-$ [c]	aq. CH_3CN	0.34				[46]
	CH_3CN	0.44				this work
$[Fe(C_5H_4CO_2H)_2]$	DMF	0.80 (0.10)				this work

[a] The CV's were recorded at ambient temperature using 0.10 M $[nBu_4N][PF_6]$ as supporting electrolyte at a scan rate of 100 mV s^{-1}. The data refer to the perchlorate salts. Sample concentration was ca. 1.0×10^{-3} M. All potentials are referenced versus the saturated calomel electrode (SCE). [b] Separation between the anodic (E^{pa}) and cathodic peaks (E^{pc}) of the redox wave ($\Delta E_p = E^{pa} - E^{pc}$). [c] Sodium salt. [d] Peak-potential value for irreversible processes.

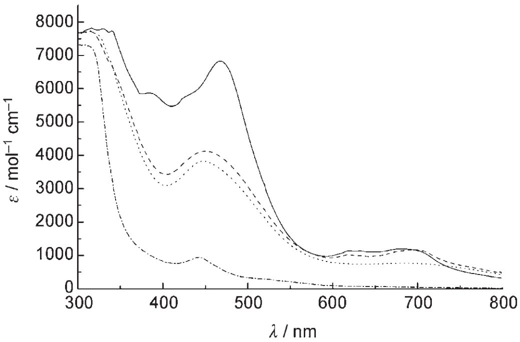

Figure 6. UV/Vis spectra of **6** (–•–•), $\mathbf{6}^{2+}$ (•••••), $\mathbf{6}^{3+}$ (-----), and $\mathbf{6}^{4+}$ (——) in acetonitrile generated by chemical oxidation of [LCo$^{II}_2$(μ-O$_2$CC$_5$H$_4$FeCp)][ClO$_4$] (**6**[ClO$_4$]) with 0.5, 1.0, and 1.5 equiv of Br$_2$, respectively.

stable on the time scale of a cyclic voltammetry experiment. Attempts to prepare these compounds by electrochemical or chemical oxidation led to unidentified decomposition products. Thus, while some of the above oxidations appear electrochemically reversible, they are all chemically irreversible.

Of the tetranuclear complexes, only complex **11**[ClO$_4$]$_4$ had sufficient solubility (due to its higher charge) to examine its electrochemical properties by cyclic voltammetry. The CV shows two quasi-reversible redox waves. On the basis of the crystal-structure of **11**[ClO$_4$]$_4$, the first redox wave at 0.22 V can be assigned to a two-electron reduction of $\mathbf{11}^{4+}$ yielding the fully-reduced Co$^{II}_4$Fe form $\mathbf{11}^{2+}$ (which is assumed to be identical with **9**). The other wave at 0.53 V can be attributed to a metal-centred two-electron oxidation process yielding the fully oxidized Co$^{III}_4$Fe form [(LCo$^{III}_2$)$_2$(Fe(Cp))]$^{6+}$ ($\mathbf{11}^{6+}$). The observed potential values are almost identical with those in **4**,[23] indicating that the oxidation/reduction processes at one [LCo$_2$] unit do not influence the ones that occur at the other. In other words, the two dinuclear cobalt(II) subunits behave as two independent redox-groups. That is fully consistent with the large distance between the two subunits and the fact that the electrostatic (Coulomb) interactions decrease rapidly with increasing distance between the redox sites. The redox wave for the oxidation of the [Fe(C$_5$H$_4$CO$_2$)$_2$]$^{2-}$ unit in **11** could not be detected. We assume that it is obscured by the redox waves at 0.53 V.

There have been many reports in the literature that a charged subunit can influence the redox properties of an adjacent ferrocene group;[47] to our knowledge, complexes **6–8** represent the first examples for a system in which the redox properties of a ferrocenecarboxylate-based ligand is modified by dinuclear aminethiophenolate complexes.

Magnetic properties of complex 10[BPh$_4$]$_2$: The magnetic properties of the pentanuclear Ni$_4$Fe complex **10**[BPh$_4$]$_2$ were examined in view of literature reports that conjugated dicarboxylate ligands can mediate long-range magnetic exchange interactions.[48] Figure 7 displays the temperature dependence of the effective magnetic moment for **10**[BPh$_4$]$_2$.

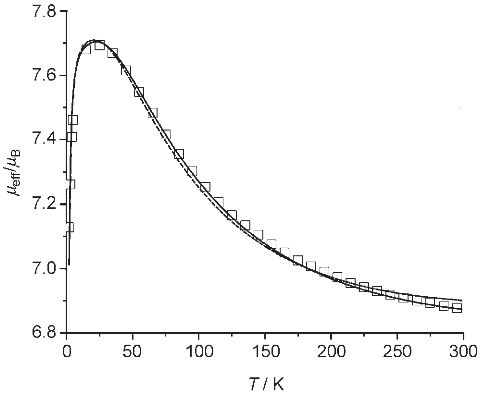

Figure 7. Temperature dependence of μ$_{eff}$ (per tetranuclear complex) for **10**[BPh$_4$]$_2$. The full line represents the best theoretical fit to Equation (1). The dashed line represents the best fit to the dimer model in Equation (3). Experimental and calculated values are provided as Supporting Information.

The effective magnetic moment increases from 6.88 μ$_B$ at 295 K to a maximum value of 7.70 μ$_B$ at 25 K. On lowering the temperature further the magnetic moment decreases to 7.08 μ$_B$ at 2 K. Although the effective magnetic moment at 25 K is smaller than expected for the spin-only value of 9.84 μ$_B$ for $S_T = 4$ resulting from the ferromagnetic coupling of four Ni^{II} ions ($S_i = 1$, $g = 2.20$), it is larger than the value of 6.22 μ$_B$ calculated for four noninteracting Ni^{II} ions. This behaviour indicates the presence of weak ferromagnetic exchange interactions between the Ni^{II} ions in the binuclear subunits but negligible—if any—coupling across the metallocene dicarboxylate bridge. Considering the long distance between the nickel(II) ions, this is not surprising.

To determine the magnitude of the exchange interactions, the magnetic susceptibility data were simulated by using Equation (1), where χ_{tetra} and χ_{mono} refer to the molar susceptibilities of a Ni$_4$ complex and a fraction ρ of a mononuclear nickel(II) impurity with Curie constant $C = Ng^2\mu_B{}^2/3kT$.

$$\chi = \chi_{\text{tetra}}(1-\rho) + 4\chi_{\text{mono}}\rho \qquad (1)$$

The molar magnetic susceptibility χ_{tetra} was derived from the appropriate spin-Hamiltonian [Eq. (2)] including the isotropic HDVV exchange, the single-ion zero-field splitting and the single-ion Zeeman interaction by a full-matrix diagonalization approach.[49]

$$H = -2J_1(\hat{S}_1\cdot\hat{S}_2+\hat{S}_3\cdot\hat{S}_4)-2J_2(\hat{S}_1\cdot\hat{S}_3+\hat{S}_1\cdot\hat{S}_4+\hat{S}_2\cdot\hat{S}_3+\hat{S}_2\cdot\hat{S}_4)+\sum_{i=1}[D_i(\hat{S}_{iz}^2-{}^1\!/_3S_i(S_i+1))+g_i\mu_B S_{i\tau}B_\tau] \quad (\tau = x, y, z) \qquad (2)$$

In this model J_1 represents the exchange interaction between the nickel ions in the binuclear subunit, whereas J_2 describes the interaction across the metallocene carboxylate linker. To reduce the number of variables the D and g

values were considered to be identical for the four nickel atoms. Under these conditions the fitting parameters were found to be $J_1=22.01\ \text{cm}^{-1}$, $J_2=0.027\ \text{cm}^{-1}$, $g=2.22$, $D=-7.62\ \text{cm}^{-1}$, and $\rho=0.02\,\%$. The inclusion of the D parameter improved the low-temperature fit significantly, but it represents by no means an accurate value (temperature dependent magnetic susceptibility measurement are not very appropriate for the determination of the sign and magnitude of D).[50,51] Nevertheless, it is clear that magnetic exchange interactions via the metallocene dicarboxylate linker are not significant ($J_2 \approx 0\ \text{cm}^{-1}$); the magnetic properties of the tetranuclear systems are solely based on the exchange couplings in the binuclear $[\text{LNi}_2(\text{O}_2\text{CR})]^+$ subunits. In this respect, we also tried to simulate the temperature dependence of the magnetic data by using an isotropic dimer model [Eq. (3)] for two Ni$^{\text{II}}$ (S = 1) ions based on the Hamiltonian in Equation (4). The magnetic data could be reproduced equally well by this approach (dashed line in Figure 7), yielding $J=22.74\ \text{cm}^{-1}$, $g=2.21$, $D=-4.29\ \text{cm}^{-1}$, and $\rho=0.03\,\%$. Again, this analysis establishes a weak ferromagnetic coupling between the two Ni$^{\text{II}}$ ions. The values are typical for carboxylato-bridged nickel(II) complexes supported by L^{2-}.[20]

$$\chi = 2[\chi_{\text{dim}}(1-\rho) + 2\chi_{\text{mono}}\rho] \tag{3}$$

$$H = -2JS_1S_2 + \sum_{i=1}^{2} (D_i(\hat{S}_{zi}^2 - {}^1\!/\!_3(S_i(S_i+1)) + g_i\mu_\text{B} S_{i\tau}B_\tau))$$

$$(\tau = x, y, z)$$

Conclusion

In summary, we presented the synthesis and characterization of the first members of a new class of polynuclear transition metal complexes composed of classical [LM$_2$] units (M = Co, Ni, Zn, L = macrocyclic hexaazadithiophenolate ligand) and ferrocenylcarboxylate groups. The complexes are readily prepared and exist as stable and discrete complexes in the solution and solid state as ascertained by various spectroscopic methods and X-ray crystallography. All complexes were found to exhibit a rich redox chemistry. Complexation of the ferrocenylcarboxylates by the LM$_2$ fragments results in large potential shifts of the ferrocenyl-centred redox process. The redox processes of the LM$_2$ units are also affected upon complex formation, showing that the electron transfer events of the ferrocenyl moiety and the binuclear subunit influence one another. In **11**, however, the two dinuclear cobalt(II) subunits behave as two independent redox-groups owing to the large distance between them. Additionally, we found that the magnetic properties in the pentanuclear Ni$_4$Fe complex **10** are based on the ferromagnetic exchange interactions between the Ni$^{\text{II}}$ ions in the binuclear subunits. The coupling across the metallocene dicarboxylate bridge is negligible. These results can now be used as a guide for further studies aimed at the synthesis of polynuclear complexes with novel electronic and magnetic properties.

Experimental Section

General comments: All solvents were dried using appropriate drying agents, distilled before use, and stored under dinitrogen. Reactions were performed under an argon atmosphere using standard Schlenk techniques. The compounds [LCo$_2$Cl][ClO$_4$] (**1**[ClO$_4$]),[23] [LNi$_2$Cl][ClO$_4$] (**2**-[ClO$_4$]),[18] and [LZn$_2$(OAc)][ClO$_4$] (**3**[ClO$_4$])[22] were prepared as described in the literature. Ferrocenecarboxylic acid and 1,1′-ferrocenedicarboxylic acid were purchased from Aldrich. Melting points were determined in capillaries and are uncorrected. IR spectra were taken on a Bruker VECTOR 22 FT-IR-spectrophotometer as KBr pellets. Electronic absorption spectra were recorded on a Jasco V-570 UV/Vis/near IR spectrophotometer. Cyclic voltammetry measurements were carried out at 25 °C with an EG&G Princeton Applied Research potentiostat/galvanostat model 263 A. The cell contained a Pt working electrode, a Pt wire auxiliary electrode, and a Ag wire reference electrode. Concentrations of solutions were 0.10 M in supporting electrolyte [nBu$_4$N][PF$_6$] and ca. 1.0×10^{-3} M in sample. Cobaltocenium hexafluorophosphate [Cp$_2$Co][PF$_6$] was used as internal standard. Under our experimental conditions, the couple cobaltocenium/colbaltocene is at $E_{1/2}=-1.345$ V versus the ferrocenium/ferrocene couple (i.e., −0.945 V versus SCE). All measured potentials were converted to the SCE reference using tabulated values.[52] The temperature-dependent (295–2 K) magnetic susceptibility measurements were carried out on a SQUID magnetometer (MPMS Quantum Design) over the temperature range 2–295 K in an external magnetic field of 0.2 T. The observed susceptibility data were corrected for the underlying diamagnetism by the use of tabulated Pascal's constants.

CAUTION! *Perchlorate salts of transition metal complexes are hazardous and may explode. Only small quantities should be prepared and great care taken.*

[LCo$^{\text{II}}_2$(O$_2$CC$_5$H$_4$FeCp)][ClO$_4$] (6[ClO$_4$]): Triethylamine (101 mg, 1.00 mmol) was added to a solution of ferrocenecarboxylic acid (230 mg, 1.00 mmol) in methanol (40 mL). To this solution was added **1**[ClO$_4$] (277 mg, 0.300 mmol), and the reaction mixture was stirred for 12 h to give a pale red-brown solution. A solution of LiClO$_4$·3H$_2$O (320 mg, 2.00 mmol) in methanol (5 mL) was added to give a red-brown solid which was isolated by filtration, washed with a small amount of cold methanol, and dried in air. The crude product was recrystallized from acetonitrile/ethanol 1:1 (260 mg, 78 %). M.p. 264–266 °C (decomp); IR (KBr): $\tilde{\nu}=3053$ (w), 3023 (w), 2993 (m), 2959 (s), 2952 (s), 2898 (m), 2864 (m), 2805 (m), 1566 (s, ν_{asym}[O$_2$CR]), 1471 (s), 1454 (vs), 1435 (w, ν_{sym}[O$_2$CR]), 1388 (s), 1361 (s), 1346 (w), 1304 (w), 1283 (m), 1267 (w), 1249 (m), 1228 (m), 1199 (w), 1157 (m), 1100 (vs, ν_3[ClO$_4^-$]), 1055 (m), 1028 (m), 1006 (w), 996 (w), 977 (w), 942 (m), 930 (m), 913 (m), 899 (m), 881 (m), 815 (s), 801 (s), 787 (s), 756 (m), 744 (m), 684 (w), 670 (w), 628 (s, ν_4[ClO$_4^-$]), 578 (w), 558 (w), 515 (s), 491 (m) cm^{-1}; UV/Vis (MeCN): $\lambda_{\max}$ (ε) = 442 (939), 523 (sh, 282), 546 (sh, 225), 1250 nm (40 M^{-1} cm^{-1})); elemental analysis calcd (%) for C$_{49}$H$_{73}$ClCo$_2$FeN$_6$O$_6$S$_2$·H$_2$O (1115.44 + 18.02): C 51.92, H 6.67, N 7.41, S 5.66; found: C 52.14, H 6.78, N 7.40, S 5.20.

[LCo$^{\text{II}}_2$(O$_2$CC$_5$H$_4$FeCp)][BPh$_4$] (6[BPh$_4$]): A solution of NaBPh$_4$ (0.342 g, 1.00 mmol) in methanol (2 mL) was added to a solution of **6**[ClO$_4$] (0.112 g, 0.100 mmol) in methanol (50 mL) to give a brown-red solid, which was collected by filtration, washed with methanol, and dried in air (115 mg, 86 %). M.p. 328–330 °C (decomp); IR (KBr): $\tilde{\nu}=3054$ (m), 3030 (m), 2998 (m), 2978 (m), 2963 (s), 2952 (sh), 2899 (m), 2867 (s), 2804 (w), 1566 (s, ν_{asym}[O$_2$CR]), 1476 (s), 1456 (s), 1425 (w, ν_{sym}[O$_2$CR]), 1394 (s), 1361 (s), 1350 (w), 1306 (w), 1289 (vw), 1266 (m), 1232 (m), 1199 (m), 1177 (w), 1155 (m), 1128 (m), 1105 (m), 1077 (s), 1055 (s), 1042 (s), 1030 (m), 1003 (m), 978 (w), 928 (m), 912 (m), 881 (m), 841 (m), 822 (m), 814 (m), 803 (m), 786 (m), 744 (m), 733 (s), 705 (s, ν[BPh$_4^-$]), 626 (m), 611 (m), 577 (w), 560 (w), 544 (w), 514 (m) cm^{-1}; UV/Vis (MeCN): $\lambda_{\max}$ (ε) = 443 (931), 522 (sh, 231), 545 sh (179), 1250 nm (33 M^{-1} cm^{-1}); elemental analysis calcd (%) for $C_{73}H_{93}BCo_2FeN_6O_2S_2$ (1335.21): C 65.67, H 7.02, N 6.29; S 4.80; found C 65.44, H 6.89, N 6.07, S 4.56.

$[LNi^{II}_2(O_2CC_5H_4FeCp)][ClO_4]$ (7[ClO$_4$]): Triethylamine (101 mg, 1.00 mmol) was added to a solution of ferrocenecarboxylic acid (230 mg, 1.00 mmol) in methanol (40 mL). To the clear solution was added solid **2**-[ClO$_4$] (276 mg, 0.300 mmol) in one portion. The reaction mixture was stirred for 12 h to give a pale-green solution. A solution of $LiClO_4{\cdot}3H_2O$ (321 mg, 2.00 mmol) in methanol (5 mL) was added. The resulting green solid was isolated by filtration, washed with a small amount of cold methanol, and recrystallized from acetonitrile/ethanol 1:1 of the product as green crystals (280 mg, 84%). M.p. 270–272 °C (decomp); IR (KBr): $\tilde{\nu}$ = 3443 (s, br), 3094 (m), 2961 (s), 2952 (s), 2899 (s), 2865 (s), 2805 (w), 1571 (s, ν_{asym}[O$_2$CR]), 1468 (vs), 1397 (s), 1384 (m), 1361 (m), 1348 (w), 1307 (w), 1263 (m), 1233 (m), 1201 (m), 1170 (w), 1153 (w), 1100 (vs, ν_3-[ClO$_4^-$]), 1039 (m), 1021 (m), 1000 (m), 983 (m), 930 (m), 912 (m), 881 (m), 826 (s), 817 (w), 791 (s), 753 (w), 625 (s, ν_4[ClO$_4^-$]), 563 (w), 516 (m) cm^{-1}; UV/Vis (MeCN): λ_{max} (ε) = 449 sh (367), 649 (90), 1112 nm (111 M^{-1} cm^{-1}).

$[LNi^{II}_2(O_2CC_5H_4FeCp)][BPh_4]$ (7[BPh$_4$]): To a stirred solution of **7**[ClO$_4$] (0.111 g, 0.100 mmol) in methanol (50 mL) was added an excess of $NaBPh_4$ (0.342 g, 1.00 mmol) dissolved in methanol (2 mL) at room temperature to give **7**[BPh$_4$] as a green powder after filtration, washing with methanol, and drying in air (122 mg, 91%). M.p. 328–330 °C (decomp); IR (KBr): $\tilde{\nu}$ = 3053 (w), 3031 (w), 2996 (m), 2979 (m), 2963 (m), 2952 (m), 2899 (m), 2867 (m), 2804 (m), 1571 (s, ν_{asym}[O$_2$CR]), 1475 (sh), 1462 (vs), 1425 (w, ν_{sym}[O$_2$CR]), 1411 (w), 1397 (s), 1384 (w), 1361 (s), 1350 (w), 1306 (w), 1289 (vw), 1264 (m), 1231 (m), 1199 (m), 1170 (w), 1151 (m), 1130 (m), 1105 (m), 1076 (s), 1058 (s), 1040 (s), 1021 (w), 999 (m), 982 (w), 930 (m), 910 (m), 881 (m), 841 (sh), 825 (w), 818 (w), 810 (w), 791 (w), 748 (w), 733 (s), 705 (s, ν[BPh$_4^-$]), 628 (m), 613 (m), 583 (w), 562 (w), 542 (w), 533 (w), 520 (m) cm^{-1}; UV/Vis (MeCN): λ_{max} (ε) = 456 sh (303), 648 (92), 1110 nm (110 M^{-1} cm^{-1}); elemental analysis calcd (%) for $C_{73}H_{93}BFeN_6Ni_2O_2S_2{\cdot}H_2O$ (1334.73 + 18.02): C 64.81, H 7.08, N 6.21, S 4.74; found: C 64.93, H 7.44, N 6.13, S 4.33.

$[LZn^{II}_2(O_2CC_5H_4FeCp)][ClO_4]$ (8[ClO$_4$]): To a solution of ferrocenecarboxylic acid (115 mg, 0.500 mmol) in methanol (40 mL) was added triethylamine (51 mg, 0.50 mmol), followed by a sample of the dizinc compound **3**[ClO$_4$] (192 mg, 0.200 mmol). After stirring for 2 d, excess $LiClO_4{\cdot}3H_2O$ (320 mg, 2.00 mmol) dissolved in methanol (5 mL) was added, to give a pale-yellow solid which was collected by filtration, washed with methanol, and dried in air. This material was treated again with a ten-fold molar excess of [HNEt$_3$][Fe(Cp)(CpCO$_2$)] as described above to ensure complete transformation of **3** into **8**. The crude product was further purified by recrystallization from ethanol/acetonitrile 1:1 to give a pale-yellow microcrystalline powder, after filtration, washing with a little cold methanol, and drying in air (167 mg, 74%). M.p. 300–301 °C (decomp); ^{1}H NMR (300 MHz, CD$_3$CN, 295 K): δ = 6.95 (s, 4H; Ar*H*), 4.40 (d, ^2J(H,H) = 11.6 Hz, 4H; ArC*H*$_2$), 4.04 (t, ^3J(H,H) = 1.9 Hz, 2H; *ortho*-C$_5$H$_4$CO$_2$), 3.90 (t, ^3J(H,H) = 1.9 Hz, 2H; *meta*-C$_5$H$_4$CO$_2$), 3.49 (dt, ^3J(H,H) = 13.7, 2.9 Hz, 4H; NC*H*HCH$_2$N), 3.40 (s, 5H; C$_5$*H*$_5$), 3.24 (dt, ^3J(H,H) = 14.0, 3.7 Hz, 4H; NCH*H*CH$_2$N), 2.87 (s, 6H; NC*H*$_3$), 2.77 (dd, ^3J(H,H) = 13.9, 3.2 Hz, 4H; NCH$_2$C*H*HN), 2.63 (d, ^2J(H,H) = 11.6 Hz, 4H; ArC*H*$_2$), 2.53 (s, 12H; NC*H*$_3$), 2.39 (dd, ^3J(H,H) = 14.0, 3.4 Hz, 4H; NCH$_2$CH*H*N), 0.93 ppm (s, 18H; *t*Bu); ^{13}C{^{1}H} NMR (75 MHz, CD$_3$CN, 295 K): δ = 174.7 (CO), 146.4 (C), 143.3 (C), 135.5 (CH), 129.2 (C), 77.8, 70.4, 70.3 (all η^5-C$_5$H$_4$CO$_2$), 69.6 (η^5-C$_5$H$_5$), 64.9 (CH$_2$), 60.0 (CH$_2$), 58.6 (CH$_2$), 50.1 (NCH$_3$), 46.0 (NCH$_3$), 34.4 (C), 31.5 ppm (CH$_3$); IR (KBr): $\tilde{\nu}$ = 3094 (w), 3045 (w), 2957 (s), 2900 (m), 2867 (m), 2809 (m), 1564 (s, ν_{asym}[O$_2$CR]), 1465 (s), 1397 (s), 1384 (m), 1361 (s), 1348 (w), 1305 (w), 1293 (w), 1266 (m), 1232 (m), 1202 (m), 1171 (m), 1154 (m), 1104 (vs, ν_3-[ClO$_4^-$]), 1054 (m), 1044 (s), 1022 (w), 1002 (m), 985 (w), 927 (m), 911 (m), 883 (m), 823 (s), 807 (s), 796 (m), 785 (m), 750 (m), 691 (w), 666 (w), 623 (s, ν_4[ClO$_4^-$]), 600 (m), 579 (w), 560 (m), 516 (s), 488 (m) cm^{-1}; UV/Vis (MeCN): λ_{max} (ε) = 342 sh (223), 440 nm (170 M^{-1} cm^{-1}); elemental analysis calcd (%) for $C_{49}H_{73}ClFeN_6O_6S_2Zn_2$ (1128.35): C 52.16, H 6.52, N 7.45, S 5.68; found: C 51.87, H 6.50, N 7.18, S 5.44.

$[(LCo^{II}_2)_2(O_2CC_5H_4)_2Fe][ClO_4]_2$ (9[ClO$_4$]$_2$): To a solution of ferrocene-1,1′-dicarboxylic acid (69 mg, 0.25 mmol) in methanol (30 mL) was added triethylamine (50 mg, 0.50 mmol). Complex **1**[ClO$_4$] (461 mg, 0.500 mmol) was added in small portions with good stirring, and the resulting brown-red suspension was stirred overnight. Further $LiClO_4{\cdot}3H_2O$ (160 mg, 1.00 mmol) in methanol (2 mL) was added to drive the precipitation to completion. The crude product was obtained as a brown-red powder after suction filtration, washing cold ethanol, and drying in air (455 mg, 89%). M.p. 336–338 °C (decomp); IR (KBr): ν = 3422 (vs), 2962 (s), 2867 (s), 2354 (w), 1634 (w), 1571 (s, ν_{asym}[O$_2$CR$^-$]), 1465 (s), 1386 (m, ν_{sym}[O$_2$CR$^-$]), 1358 (m), 1306 (w), 1265 (w), 1233 (w), 1202 (w), 1120 (s), 1092 (vs, ν_3[ClO$_4^-$]), 931 (w), 912 (w), 883 (w), 817 (m), 784 (w), 754 (w), 625 (s, ν_4[ClO$_4^-$]), 520 cm^{-1} (w); elemental analysis calcd (%) for $C_{88}H_{136}Cl_2Co_4FeN_{12}O_{12}S_4$ (2044.84): C 51.69, H 6.70, N 8.22, S 6.27; found: C 51.60, H 6.58, N 8.13, S 6.12.

$[(LCo^{II}_2)_2(O_2CC_5H_4)_2Fe][BPh_4]_2$ (9[BPh$_4$]$_2$): To a suspension of **9**[ClO$_4$]$_2$ (102 mg, 0.050 mmol) in acetonitrile (50 mL) was added a solution of $NaBPh_4$ (34.2 mg, 0.100 mmol) in ethanol (50 mL), and the resulting red-brown suspension was stirred for 2 d. The precipitate was collected by filtration, washed with ethanol, and dried in air (70 mg, 56%). M.p. 320–322 °C (decomp); IR (KBr): ν = 3443 (w), 3052 (m), 3032 (m), 2963 (s), 2897 (m), 2867 (m), 2805 (w), 1812 (w), 1768 (w), 1696 (w), 1568 (s, ν_{asym}-[O$_2$CR]), 1461 (s), 1425 (s, ν_{sym}[O$_2$CR]), 1393 (s), 1358 (s), 1306 (m), 1265 (m), 1233 (m), 1201 (w), 1169 (w), 1154 (m), 1078 (s), 1043 (s), 998 (w), 929 (w), 910 (m), 882 (m), 824 (s), 807 (m), 781 (w), 732 (s, ν[BPh$_4^-$]), 704 (s, ν[BPh$_4^-$]), 627 (m), 612 (s), 561 (w), 523 (m), 489 (w), 410 cm^{-1} (w); UV/Vis (CH$_3$CN): λ_{max} (ε) = 448 (1287), 463 (sh, 1088), 525 (439), 543 (sh, 343), 569 (sh, 199), 1255 nm (90 M^{-1} cm^{-1}); elemental analysis calcd (%) for $C_{136}H_{176}B_2Co_4FeN_{12}O_4S_4$ (2484.39): C 65.75, H 7.14, N 6.77, S 5.16; found: C 65.34, H 7.12, N 7.02, S 4.72.

$[(LNi^{II}_2)_2(O_2CC_5H_4)_2Fe][ClO_4]_2$ (10[ClO$_4$]$_2$): Triethylamine (50 mg, 0.50 mmol) was added to a solution of 1,1′-ferrocenedicarboxylic acid (69 mg, 0.25 mmol) in methanol (30 mL). Complex **2**[ClO$_4$] (461 mg, 0.500 mmol) was added, and the resulting green suspension was stirred overnight. Further $LiClO_4{\cdot}3H_2O$ (160 mg, 1.00 mmol) in methanol (2 mL) was added to drive the precipitation to completion. The crude product was obtained as a green powder after suction filtration, washing with cold ethanol, and drying in air (378 mg, 74%). M.p. > 365 °C; IR (KBr): $\tilde{\nu}$ = 3044 (w), 2958 (s), 2898 (m), 2868 (s), 2806 (m), 1572 (s, ν_{asym}-[O$_2$CR]), 1463 (s), 1423 (w), 1393 (s), 1386 (sh), 1357 (m), 1347 (sh), 1307 (w), 1294 (sh), 1264 (m), 1234 (m), 1201 (m), 1170 (m), 1152 (m), 1090 (vs, ν_3[ClO$_4^-$]), 1057 (m), 1039 (s), 999 (m), 983 (w), 930 (m), 911 (m), 881 (m), 826 (s), 807 (m), 796 (m), 788 (m), 752 (m), 696 (w), 667 (w), 627 (s, ν_3[ClO$_4^-$]), 602 (m), 563 (w), 542 (w), 524 (s), 491 cm^{-1} (m).

$[(LNi^{II}_2)_2(O_2CC_5H_4)_2Fe][BPh_4]_2$ (10[BPh$_4$]$_2$): To a suspension of **10**[ClO$_4$]$_2$ (204 mg, 0.100 mmol) in acetonitrile (50 mL) was added a solution of $NaBPh_4$ (34.2 mg, 0.100 mmol) in ethanol (50 mL), and the resulting green suspension was stirred for 2 d. The precipitate was collected by filtration, washed with ethanol and dried in air (202 mg, 81%); M.p. 357–358 °C (decomp); IR (KBr): $\tilde{\nu}$ = 3444 (m), 3055 (m), 3032 (m), 2965 (s), 2900 (m), 2869 (m), 2808 (w), 1814 (w), 1616 (w), 1572 (s, ν_{asym}[O$_2$CR$^-$]), 1464 (s), 1425 (w, ν_{sym}[O$_2$CR$^-$]), 1394 (s), 1358 (s), 1307 (w), 1266 (w), 1234 (w), 1201 (w), 1170 (w), 1154 (w), 1132 (w), 1113 (w), 1079 (m), 1057 (m), 1040 (m), 999 (w), 983 (w), 931 (w), 910 (w), 881 (w), 826 (m), 809 (m), 788 (w), 733 (s, ν[BPh$_4^-$]), 705 (s, ν[BPh$_4^-$]), 669 (w), 628 (m), 613 (m), 563 (w), 526 (m), 491 (w), 416 cm^{-1} (w); UV/Vis (CH$_2$Cl$_2$): λ_{max} (ε) = 655 (72), 1112 nm (151 M^{-1} cm^{-1}); elemental analysis calcd (%) for $C_{136}H_{176}B_2FeN_{12}Ni_4O_4S_4$ (2483.43): C 65.77, H 7.14, N 6.77, S 5.16; found: C 65.54, H 7.19, N 6.94, S 5.38.

$[(LCo^{II}Co^{III})_2(O_2CC_5H_4)_2Fe][ClO_4]_4$ (11[ClO$_4$]$_4$): A solution of bromine (16.6 mg, 0.110 mmol) in acetonitrile was added dropwise to a brown-red suspension of **9**[ClO$_4$]$_2$ (204 mg, 0.100 mmol) in acetonitrile (30 mL) at 0 °C. After an ice-cold solution of $LiClO_4{\cdot}3H_2O$ (160 mg, 1.00 mmol) in EtOH (30 mL) was added to the brown-black solution, the volume of the mixture was quickly concentrated in vacuum resulting in the formation of a black microcrystalline solid that was quickly isolated by filtration, washed with cold ethanol, and dried in air (152 mg, 68%). M.p. > 365 °C; IR (KBr): $\tilde{\nu}$ = 3433 (s), 3055 (w), 2962 (s), 2905 (s), 2870 (s), 2020 (w), 1629 (m), 1557 (s, ν_{asym}[O$_2$CR]), 1464 (s), 1426 (m), 1389 (s, ν_{sym}[O$_2$CR]), 1357 (s), 1306 (w), 1264 (w), 1237 (m), 1199 (w), 1108 (vs,

Table 3. Crystallographic data for the compounds.

Compound	**6**[BPh$_4$] ·3 MeCN	**7**[BPh$_4$] ·MeCN	**9**[BPh$_4$]$_2$ ·2^2/$_3$MeCN ·^{1}/$_3$H$_2$O	**10**[BPh$_4$]$_2$ ·1.75 MeCN ·EtOH·0.25 H$_2$O	**11**[ClO$_4$]$_4$ ·4 H$_2$O
formula	$C_{79}H_{102}BCo_2FeN_9O_2S_2$	$C_{75}H_{96}BFeN_7Ni_2O_2S_2$	$C_{141.33}H_{184.67}B_2Co_4FeN_{14.67}O_{4.33}S_4$	$C_{141.50}H_{187.75}B_2FeN_{13.75}Ni_4O_{5.25}S_4$	$C_{88}H_{144}C_{14}Co_4FeN_{12}O_{24}S_4$
M_r [g mol^{-1}]	1458.34	1375.79	2599.80	2605.85	2315.76
Space group	$P\bar{1}$	$P2/c$	$P2_1/c$	$P2_1/c$	$P2/c$
a [Å]	14.384(3)	19.488(4)	17.082(3)	17.051(2)	21.900(4)
b [Å]	15.713(3)	13.245(3)	27.993(4)	27.953(4)	15.046(3)
c [Å]	19.059(4)	30.312(6)	27.942(4)	27.934(4)	33.251(7)
α [°]	101.94(4)	90.00	90.00	90.00	90.00
β [°]	110.31(3)	108.52(4)	93.98(3)	94.02(3)	94.42(3)
γ [°]	100.87(4)	90.00	90.00	90.00	90.00
V [Å^3]	3790(2)	7419(2)	13329(3)	13282(3)	10923(4)
Z	2	4	4	4	4
ρ_{calcd} [g cm^{-3}]	1.278	1.232	1.296	1.306	1.408
$\mu(Mo_{K\alpha})$ [mm^{-1}]	0.728	0.799	0.716	0.786	0.970
θ limits [°]	1.19–28.69	1.10–28.81	1.03–29.10	1.03–28.85	1.35–28.88
measured refl.	32546	65523	84486	82969	67912
independent refl.	17160	17911	32128	31656	26092
observed refl.[a]	9722	6646	6894	14584	9040
parameters	893	839	1523	1558	1278
$R1$[b] ($R1$ all data)	0.0573 (0.1084)	0.0903 (0.2166)	0.0714 (0.3243)	0.0464 (0.1387)	0.0676 (0.1910)
w$R2$[c] (w$R2$ all data)	0.1309 (0.1633)	0.2261 (0.2952)	0.1528 (0.2247)	0.0904 (0.1167)	0.1857 (0.2332)
Max, min peaks [e Å^{-3}]	0.721/−0.921	0.912/−1.559	0.761/−0.760	0.730/−0.539	1.327/−0.545
CCDC	633401	633402	633403	633404	633405

[a] Observation criterion: $I > 2\sigma(I)$. [b] $R1 = \Sigma||F_o|-|F_c||/\Sigma|F_o|$. [c] $wR2 = \{\Sigma w(F_o^2-F_c^2)^2]/\Sigma w(F_o^2)^2]\}^{1/2}$.

ν_3[ClO$_4^-$]), 1037 (s), 932 (w), 910 (w), 885 (m), 825 (m), 809 (m), 790 (w), 754 (w), 738 (w), 706 (w), 625 (s, ν_4[ClO$_4^-$]), 565 (m), 531 (m), 489 (m), 437 (w), 423 cm^{-1} (w); UV/Vis (CH$_3$CN): λ_{max} (ε)=449 (5242), 681 nm (1091 M^{-1} cm^{-1}); elemental analysis calcd (%) for $C_{88}H_{136}Cl_4Co_4FeN_{12}O_{20}S_4 \cdot 4H_2O$ (2243.7+72.06): C 45.64, H 6.27, N 7.26, S 5.54; found: C 45.50, H 6.44, N 7.26, S 6.66. Crystals of **11**[ClO$_4$]$_4$ suitable for X-ray crystallography were selected from the mother liquor.

Collection and reduction of X-ray data: Table 3 summarizes the crystallographic data for **6**[BPh$_4$]·3 MeCN, **7**[BPh$_4$]·MeCN, **9**[BPh$_4$]$_2$·2^2/$_3$MeCN·^{1}/$_3$H$_2$O, **10**[BPh$_4$]$_2$·1.75 MeCN·EtOH·0.25 H$_2$O, and **11**[ClO$_4$]·4 H$_2$O. The crystals were mounted on the tip of a glass fiber using perfluoropolyether oil. Intensity data were collected at 210(2) K, using a Bruker SMART CCD diffractometer. Graphite monochromated Mo$_{K\alpha}$ radiation (λ=0.71073 Å) was used throughout. The data were processed with SAINT and corrected for absorption using SADABS.[53] Structures were solved by direct methods[54] and refined by full-matrix least-squares on the basis of all data against F^2 using SHELXL-97.[55] PLATON was used to search for higher symmetry.[56] H atoms were placed at calculated positions and refined as riding atoms with isotropic displacement parameters. All non-hydrogen atoms were refined anisotropically, except those of some disordered solvate molecules.

In **6**[BPh$_4$]·3 MeCN and **7**[BPh$_4$]·MeCN a *tert*-butyl group was found to be rotationally disordered over two sites. In **6** the two orientation were freely refined by using a split atom model to give site occupancies of 0.54(2) (C(36a)–C(38a)) and 0.46(2) (C(36b)–C(38b)). For **7**, the disorder was refined with restrained C–C and C⋯C distances applying the SADI-instructions implemented in the SHELXL program suite to give site occupancies of 0.54(3) (for (C(36a)–C(38a)) and 0.46(3) (for (C(36b)–C(38b))), respectively. Some of the solvate molecules in **9**[BPh$_4$]$_2$·2^2/$_3$MeCN·^{1}/$_3$H$_2$O and **10**[BPh$_4$]$_2$·1.75 MeCN·EtOH·0.25 H$_2$O were found to be severely disordered and/or partially occupied. In **9**[BPh$_4$]$_2$·2^2/$_3$MeCN·^{1}/$_3$H$_2$O one solvent site was found to be occupied partially by acetonitrile and water molecules. The occupancy factors of these molecules were fixed at ^{2}/$_3$ and ^{1}/$_3$, respectively, and the C, N, and O atoms were refined isotropically. Similarly, in **10**[BPh$_4$]$_2$·1.75 MeCN·EtOH·0.25 H$_2$O one solvent site was found to be occupied partially by an acetonitrile (s.o.f(fixed)=0.75) and a water molecule (s.o.f(fixed)=0.25)) molecules. In both structures, water hydrogen atoms were not included in the refinements. One of the ClO$_4^-$ anions and all four water molecules in **11**[ClO$_4$]$_4$·4 H$_2$O were found to be disordered over two sites. Another ClO$_4^-$ ions was disordered over three distinct sites in a 33:33:33 % ratio. The various Cl–O and O⋯O distances were restrained using the SADI instructions implemented in the SHELXL program suite and the Cl and O atoms of one anion ClO$_4^-$ could only be refined with isotropic thermal parameters. Again, no hydrogen atoms were calculated for the disordered water molecules. Graphics were obtained with ORTEP 3 for Windows.[57]

CCDC-633401–633405 contains the supplementary crystallographic data for this paper. These data can be obtained free of charge from The Cambridge Crystallographic Data Centre via www.ccdc.cam.ac.uk/data_request/cif

Acknowledgements

We are grateful to Professor H. Vahrenkamp for providing facilities for NMR and X-ray crystallographic measurements. Financial support from the Deutsche Forschungsgemeinschaft (SPP 1137 "Molecular Magnetism", KE 585/4-3,2,1) and the Universät Leipzig is gratefully acknowledged.

[1] *Ferrocenes* (Eds.: A. Togni, T. Hayashi), VCH, Weinheim, **1995**.

[2] a) F. A. Cotton, J. P. Donahue, C. A. Murillo, *Inorg. Chem.* **2001**, *40*, 2229–2233; b) F. A. Cotton, C. Lin, C. A. Murillo, *Inorg. Chem.* **2001**, *40*, 478–484.

[3] D. Astruc, *Electron Transfer and Radical Processes in Transition-Metal Chemistry*, Wiley-VCH, Weinheim, **1995**.

[4] C. D. Hall, T.-K.-U. Truong, J. H. R. Tucker, J. W. Steed, *Chem. Commun.* **1997**, 2195–2196.

[5] a) A. M. DeBlass, C. DeSantis, L. Fabrizzi, M. Liccheli, P. Pallavicini, A. Poggi, in *Supramolecular Chemistry* (Eds.: V. Balzani, L.

DeCola), Kluwer Academic Publishers, London, **1995**, 87–93; b) J. W. Steed, J. L. Atwood, *Supramolecular Chemistry*, Wiley, Chichester, **2000**, 224–230, 574–639.

[6] S. D. Christie, S. Subramanian, L. K. Thomson, M. J. Zaworotko, *Chem. Commun.* **1994**, 2563–2564.

[7] N. Metzler-Nolte, K. Severin, in *Concepts and Models in Bioinorganic Chemistry* (Eds.: H.-B. Kraatz, N. Metzler-Nolte), Wiley-VCH, Weinheim, **2006**, 113–133.

[8] T. Matsue, D. H. Evans, T. Osa, N. Kobayashi, *J. Am. Chem. Soc.* **1985**, *107*, 3411–3417.

[9] a) P. D. Beer, *Chem. Commun.* **1996**, 689–696; b) P. D. Beer, A. D. Keefe, A. M. Z. Slawin, D. J. Williams, *J. Chem. Soc. Dalton Trans.* **1990**, 3675–3682; c) P. D. Beer, *Acc. Chem. Res.* **1998**, *31*, 71–80.

[10] J. C. Medina, T. T. Goodnow, M. T. Rojas, J. L. Atwood, B. C. Lynn, A. E. Kaifer, G. W. Gokel, *J. Am. Chem. Soc.* **1992**, *114*, 10583–10595.

[11] J. L. Atwood, K. T. Holman, J. W. Steed, *Chem. Commun.* **1996**, 1401–1408.

[12] M'hamed Chahma, J. S. Lee, H.-B. Kraatz, *J. Organomet. Chem.* **2002**, *648*, 81–86.

[13] a) A. Harriman, R. Ziessel, *Chem. Commun.* **1996**, 1707–1716; b) M. Buda, J.-C. Moutet, E. Saint-Arman, A. DeCian, J. Fischer, R. Ziessel, *Inorg. Chem.* **1998**, *37*, 4146–4148; c) A. Ion, J.-C. Moutet, E. Saint-Aman, G. Royal, S. Tingry, J. Pecaut, S. Menage, R. Ziessel, *Inorg. Chem.* **2001**, *40*, 3632–3636; d) J.-C. Moutet, E. Saint-Aman, G. Royal, S. Tingry, R. Ziessel, *Eur. J. Inorg. Chem.* **2002**, 692–698.

[14] I. R. Butler, M. Kalaji, L. Nehrlich, M. Hursthouse, A. I. Karaulov, K. M. Abdul Malik, *J. Chem. Soc. Chem. Commun.* **1995**, 459–460.

[15] A. Houlton, N. Jasim, R. M. G. Roberts, J. Silver, D. Cunningham, P. McArdle, T. Higgins, *J. Chem. Soc. Dalton Trans.* **1992**, 2235–2241.

[16] P. D. Beer, J. E. Nation, S. L. W. McWhinnie, M. E. Harman, M. B. Hursthouse, M. I. Ogden, A. H. White, *J. Chem. Soc. Dalton Trans.* **1991**, 2485–2492.

[17] a) F. A. Cotton, C. Lin, C. A. Murillo, *Inorg. Chem.* **2001**, *40*, 472–477; b) F. A. Cotton, J. P. Donahue, C. Lin, C. A. Murillo, *Inorg. Chem.* **2001**, *40*, 1234–1244.

[18] B. Kersting, G. Steinfeld, *Chem. Commun.* **2001**, 1376–1377.

[19] M. H. Klingele, G. Steinfeld, B. Kersting, *Z. Naturforsch.* **2001**, *56b*, 901–907.

[20] J. Hausmann, M. H. Klingele, V. Lozan, G. Steinfeld, D. Siebert, Y. Journaux, J. J. Girerd, B. Kersting, *Chem. Eur. J.* **2004**, *10*, 1716–1728.

[21] Y. Journaux, V. Lozan, J. Hausmann, B. Kersting, *Chem. Commun.* **2006**, 83–84.

[22] B. Kersting, *Angew. Chem.* **2001**, *113*, 4110–4112; *Angew. Chem. Int. Ed.* **2001**, *40*, 3988–3990.

[23] B. Kersting, G. Steinfeld, *Inorg. Chem.* **2002**, *41*, 1140–1150.

[24] G. Steinfeld, V. Lozan, B. Kersting, *Angew. Chem.* **2003**, *115*, 2363–2365; *Angew. Chem. Int. Ed.* **2003**, *42*, 2261–2263.

[25] Y. Journaux, T. Glaser, G. Steinfeld, V. Lozan, B. Kersting, *Dalton Trans.* **2006**, 1738–1748.

[26] M. R. Churchill, Y.-J. Li, D. Nalewajek, P. M. Schaber, J. Dorfman, *Inorg. Chem.* **1985**, *24*, 2684–2687.

[27] R. Costa, C. Lopez, E. Molins, E. Espinosa, *Inorg. Chem.* **1998**, *37*, 5686–5689.

[28] B. Klingert, G. Rihs, *Organometallics* **1990**, *9*, 1135–1141.

[29] a) M. Gressenbuch, V. Lozan, G. Steinfeld, B. Kersting, *Eur. J. Inorg. Chem.* **2005**, 2223–2234; b) M. Gressenbuch, B. Kersting, *Eur. J. Inorg. Chem.* **2007**, 90–102.

[30] K. Nakamoto, *Infrared and Raman Spectra of Inorganic and Coordination Compounds*, 5th ed., Wiley, New York, **1997**.

[31] H. Lang, K. Köhler, L. Zsolnai, *Chem. Ber.* **1995**, *128*, 519–523.

[32] V. Lozan, B. Kersting, *Eur. J. Inorg. Chem.* **2005**, 504–512.

[33] J. Tao, W. Xiao, *J. Organomet. Chem.* **1996**, *526*, 21–24.

[34] M. Sabbatini, M. A. Franco, R. Psaro, *Inorg. Chim. Acta* **1980**, *42*, 267–270.

[35] X.-B. Wang, B. Dai, H.-K. Woo, L.-S. Wang, *Angew. Chem.* **2005**, *117*, 6176–6178; *Angew. Chem. Int. Ed.* **2005**, *44*, 6022–6024.

[36] M. B. Robin, P. Day, *Adv. Inorg. Chem. Radiochem.* **1967**, *10*, 247–422.

[37] F. Takusagawa, T. F. Koetzle, *Acta Crystallogr. Sect. B* **1979**, *35*, 1074–1081.

[38] M. W. Cooke, T. S. Cameron, K. N. Robertson, J. C. Swarts, M. A. S. Aquino, *Organometallics* **2002**, *21*, 5962–5971.

[39] M. A. S. Aquino, *Coord. Chem. Rev.* **1998**, *170*, 141–202.

[40] C. Lopez, R. Costa, F. Illas, E. Molins, E. Espinosa, *Inorg. Chem.* **2000**, *39*, 4560–4565.

[41] F. Takusagawa, T. F. Koetzle, *Acta Crystallogr. Sect. B* **1979**, *35*, 2888–2896.

[42] G. J. Palenik, *Inorg. Chem.* **1969**, *8*, 2744–2749.

[43] L. A. Tyler, J. C. Noveron, M. M. Olmstead, P. K. Mascharak, *Inorg. Chem.* **2000**, *39*, 357–362.

[44] T. C. Higgs, D. Ji, R. S. Czernuszewicz, B. F. Matzanke, V. Schünemann, A. X. Trautwein, M. Helliwell, W. Ramirez, C. J. Carrano, *Inorg. Chem.* **1998**, *37*, 2383–2392.

[45] a) F. A. Cotton, J. P. Donahue, C. A. Murillo, L. M. Perez, *J. Am. Chem. Soc.* **2003**, *125*, 5486–5492; b) M. H. Chisholm, B. D. Pate, P. J. Wilson, J. M. Zalewski, *Chem. Commun.* **2002**, 1084–1085.

[46] The electrochemical properties of $[Fe(Cp)(C_5H_4CO_2H)]$ and $[Fe(Cp)C_5H_4CO_2]^-$ have been determined by Fabrizzi and co-workers. Under their experimental conditions (i.e., 20% aqueous acetonitrile solution) $[Fe(Cp)(C_5H_4CO_2H)]$ and $[Fe(Cp)C_5H_4CO_2]^-$ undergo reversible one-electron oxidations at +0.53 and +0.33 V, respectively, see, G. De Santis, L. Fabrizzi, M. Licchelli, P. Pallavicini, *Inorg. Chim. Acta* **1994**, *225*, 239–244. Under our conditions (i.e., neat acetonitrile), the respective one-electron oxidations occur at slightly more anodic potentials at +0.62 and +0.44 V, respectively.

[47] P. D. Beer, *Chem. Soc. Rev.* **1989**, *18*, 409–450.

[48] S. Bayly, J. A. McCleverty, M. D. Ward, D. Gatteschi, F. Totti, *Inorg. Chem.* **2000**, *39*, 1288–1293.

[49] B. Kersting, G. Steinfeld, D. Siebert, *Chem. Eur. J.* **2001**, *7*, 4253–4258.

[50] T. Beissel, T. Glaser, F. Kesting, K. Wieghardt, B. Nuber, *Inorg. Chem.* **1996**, *35*, 3936–3947.

[51] K. K. Nanda, A. W. Addison, N. Paterson, E. Sinn, L. K. Thompson, U. Sakaguchi, *Inorg. Chem.* **1998**, *37*, 1028–1036.

[52] N. G. Connelly, W. E. Geiger, *Chem. Rev.* **1996**, *96*, 877–910.

[53] SADABS, An empirical absorption correction program; Part of the SAINTPlus NT version 5.10 package, BRUKER AXS, Madison, WI, **1998**.

[54] G. M. Sheldrick, *Acta Crystallogr. Sect. A* **1990**, *46*, 467–473.

[55] G. M. Sheldrick, SHELXL-97, Computer program for crystal structure refinement, University of Göttingen, Göttingen (Germany), **1997**.

[56] A. L. Spek, PLATON—A Multipurpose Crystallographic Tool, Utrecht University, Utrecht (The Netherlands), **2000**.

[57] a) L. J. Farrugia, ORTEP 3 for Windows, Version 1.05, University of Glasgow (UK), **1997**; b) L. J. Farrugia, *J. Appl. Crystallogr.* **1997**, *30*, 565.

Received: January 23, 2007